ЖЭТФ, 2010, том 137, вып. 3, стр. 590–598

STABILITY OF A DEPOSITED LIQUID CLUSTER

P. V. Kashtanov[a]*, ***R. Hippler***[b], ***B. M. Smirnov***[a]**, ***S. R. Bhattacharyya***[c]

[a] *Joint Institute for High Temperatures of Russian Academy of Sciences*
125412, Moscow, Russia

[b] *Institut für Physik, Ernst-Moritz-Arndt-Universität Greifswald*
17489, Greifswald, Germany

[c] *Saha Institute of Nuclear Physics*
700064, Kolkata, India

Received September 15, 2009

The fragmentation of silver liquid clusters deposited onto a silicon surface is observed after heating the clusters to 1073 K and subsequently annealing with the exposition time 3 min. This contradicts macroscopic models of a liquid drop deposited on a surface if we are based on critical parameters of bulk silver. Some versions are analyzed that are based on cluster properties and may explain the phenomenon of cluster fragmentation. An experiment is suggested for clarifying the nature of the cluster fragmentation phenomenon and cluster critical phenomena.

1. INTRODUCTION

Thin films consisting of metal clusters deposited on a substrate are a specific physical object [1] that is importante in device fabrication and some technological applications [2]. Along with this, it is interesting from the fundamental standpoint due to the measuring techniques that allow studying various details of this problem. In addition, silver is used as an antibacterial material, and therefore silver covering is used in various antibacterial applications [3–5]. Silver produces the strongest action on bacteria when it has a porous structure with structural elements 1–10 nm in size [6], which corresponds to the size of clusters when they are generated in a cluster source.

Metal clusters deposited on a surface are the prospective objects for applications. Development of nanotechnology based on deposited clusters gives impetus to creating a fine and expensive experimental setup that in turn allows studying the properties of deposited clusters and processes involving them. In other words, contemporary measurement tools allow studying the known physical phenomena involving nanosized particles in detail. Below, we consider the fragmentation of deposited liquid clusters located on a surface from this standpoint. We are based on experimental data for this phenomenon and are guided by simple physical models.

2. EXPERIMENTAL SETUP AND RESULTS

In the experiment, we create silver clusters in magnetron discharge, where silver clusters are formed in an argon flow [7, 8]. The flow with silver clusters expands in a vacuum through an orifice 3–6 mm in diameter, and then clusters, which are charged by a crossed electron beam, pass through a mass spectral filter constructed on the basis of a quadrupole mass spectrometer [9]. As a result, we obtain a beam of clusters 5.6 nm in diameter (approximately 4600 atoms per silver cluster), and this beam is deposited onto the silicon surface with the energy approximately given by 0.7 eV per atom. Under the used intensities of the cluster beam, solid silver clusters of the beam join into aggregates in the course of attachment to the surface.

These aggregates, fastened to the silicon surface and consisting of solid silver clusters, are subjected to rapid thermal annealing up to various temperatures in nitrogen atmosphere [10, 11] and to rapid thermal annealing with the exposition time 3 min in this experiment. The structure of deposited silver clusters is detected by a scanning electron microscope (the operating voltage is 10 kV, the magnification is 60000) with energy

---

*E-mail: kashtanov@gmail.com
**E-mail: bsmirnov@gmail.com

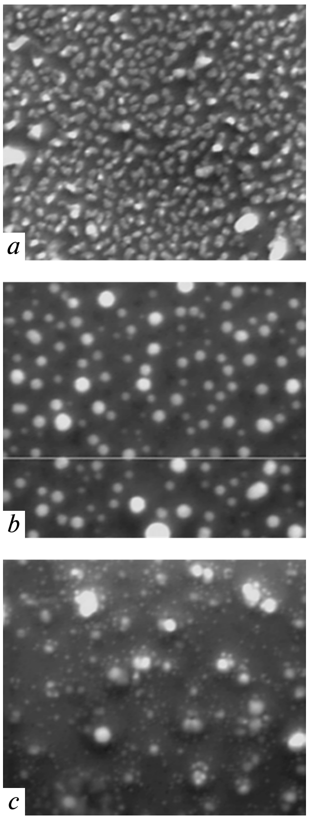

Fig. 1. The structure of a film formed by deposition of silver clusters with a diameter about 5.6 nm onto a silicon surface and subsequent rapid thermal annealing in nitrogen atmosphere with the exposition 3 min [10]. The photographs are made with a scanning electron microscope (the operating voltage is 10 kV, the magnification is 60000). The heating temperature is 673 (*a*), 873 (*b*), and 1073 (*c*) K

dispersive X-ray analysis. In addition, in order to obtain information about the cluster height, atomic force microscopy is used for the analysis of the structure of deposited clusters in the tapping mode at the resonance frequency about 428 kHz under ambient conditions. Typical photographs of the films obtained after annealing are given in Fig. 1.

The results in Fig. 1 are treated to obtain the size distribution of aggregates and drops on the substrate surface [10, 11]. A typical size of surface aggregates, which consist of incident clusters, is several times greater than the size of incident clusters [10, 11]. According to Figs. 1*b* and *c*, melting of surface aggregates leads to shortening of the volume occupied by silver, i. e., the silver aggregates are porous at the beginning. Next, the substrate (silicon) has dielectric properties. Therefore, clusters are neutral, and because they are separated from each other, interaction between nearest clusters is not essential.

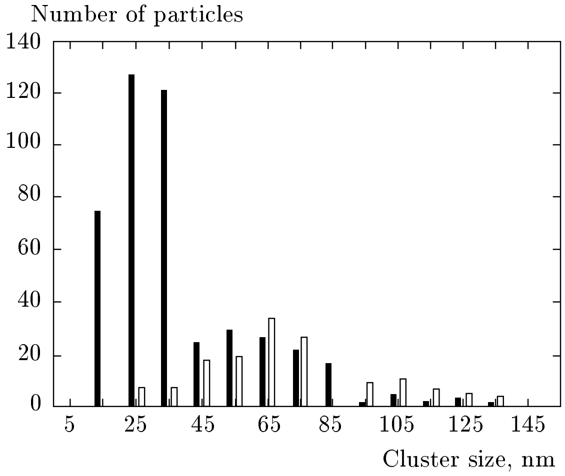

Fig. 2. The size distribution function of drops for silver deposition under the conditions in Fig. 1. The annealing temperature is 873 K (open histograms) and 1073 K (closed histograms)

In Fig. 2, guided by the phenomenon of cluster fragmentation, we give the size distribution of deposited clusters after heating up to temperatures above the cluster melting point, if deposited clusters are transformed into single drops on the substrate surface. These measurements are made with a scanning electron microscope, and hence the cluster size in Fig. 2 is the diameter of the cluster projection onto the substrate. As is seen from Fig. 2, at the heating temperature 873 K, the size distribution function of deposited clusters may be approximated by the usual Gauss distribution, while at the heating temperature 1073 K, the size distribution function becomes bimodal. This means that cluster fragmentation corresponds to formation of small drops in time when the deposited cluster drops are at a high temperature. We note that the total mass of small clusters under experimental conditions is small (9 %). In addition, cluster evaporation also proceeds at high temperatures, and the rate of this process allowed finding the atom binding energy in large liquid clusters of silver [10]. But the total mass of evaporation under the experimental conditions is also small (about 3 % of the cluster mass is evaporated). Hence, the character of fragmentation of deposited clusters can be analyzed with the cluster evaporation ignored.

According to the experimental results, the silver aggregates formed on the silicon surface as a result of the deposition of solid silver clusters 5.6 nm in diameter are melted at the heating temperature below 873 K (the melting point of bulk silver is 1233 K). Then, as follows from heating to the temperature 873 K, the distribution function of the drop diameters is approximated by the Gauss distribution with the mean drop diameter 65 nm (the number of cluster atoms is $n \approx 7.5 \cdot 10^6$). Subsequent heating to 1073 K leads to a bimodal distribution function. When approximated by the Gauss distributions, the observed distribution leads to the average cluster diameters 55 nm ($n \approx 5.5 \cdot 10^6$) and 25 nm ($n \approx 4 \cdot 10^5$). In what follows, analyzing the fragmentation of a liquid cluster located on a surface, we consider simple models for such a cluster, which allows us to find conditions for the fragmentation phenomenon to be realized.

3. THERMODYNAMICS OF A FREE LIQUID CLUSTER

We first consider the thermodynamics of a liquid cluster consisting of $n \gg 1$ atoms and located in a vacuum. The binding energy of atoms at zero temperature expanded in the small parameter $n^{-1/3}$ for a large cluster with two expansion terms kept is given by [12, 13]

$$E_b(n) = \varepsilon_0 n - A n^{2/3}, \tag{3.1}$$

where ε_0 is the binding energy per atom for a macroscopic system of bound atoms, A is the specific surface energy, related to the surface tension σ for the corresponding liquid as [13]

$$\sigma = 4\pi r_W^2 A, \tag{3.2}$$

and r_W is the Wigner–Seits radius [14, 15] for the bulk liquid. Cluster fragmentation proceeds according to the scheme

$$M_n \to M_{n-k} + M_k, \tag{3.3}$$

where M is a metallic atom. In the limit case $n \gg k$, the expended energy ΔE in this process is equal to

$$\Delta E_{nk} = E_b(n) - E_b(n-k) - E_b(k) = \\ = A k^{2/3}\left[1 - \frac{2}{3}\left(\frac{k}{n}\right)^{1/3}\right] \approx A k^{2/3}, \quad k \ll n. \tag{3.4}$$

This is the expansion of the expended cluster energy at zero temperature over a small parameter $(k/n)^{1/3}$. As can be seen, the fragmentation of a liquid cluster is not favorable energetically.

We now analyze thermodynamic equilibrium with respect to fragmentation at a finite temperature T for a liquid cluster located on a surface. We use the Saha formula for clusters participating in process (3.3). Reducing the Saha formula [16] to the case where clusters are located on a planar surface, i. e., to a two-dimensional space, we have

$$\frac{N_{n-k} N_k}{N_n} = S(n,k) \exp\left(-\frac{\Delta E_{nk}}{T}\right) = \\ = S(n,k) \exp\left(-\frac{A k^{2/3}}{T}\right), \tag{3.5}$$

where ΔE_{nk} is given by formula (3.4), T is the temperature expressed in energy units, N_p is the number density of clusters consisting of p atoms, and the pre-exponent S in the two-dimensional case $S \backsim k$. As follows from this formula, in the case $k \gg 1$ under consideration, relation (3.5) leads to a small probability of fragmentation when clusters occupy a large part of the surface. This formula testifies to a low probability of the fragmentation of deposited liquid clusters located on a surface as long as the specific surface energy A is small. Hence, this process is possible only near the critical point if the specific surface energy A becomes very small.

We estimate the conditions of the above experiment when silver clusters are deposited onto a silicon substratum. At the melting point, $A = 2.0$ eV for silver [13, 17], and at the temperature 1073 K, $A/T \approx 22$ under the assumption that the critical temperature is higher than this one. It follows that the fragmentation observed in the above experiment and represented in Fig. 2 is impossible far from the critical point. We note that critical parameters of bulk silver corresponds to a high critical temperature (about 7000 K) and pressure ($4.5 \cdot 10^8$ Pa) [18]. These parameters correspond to the conditions under which the difference between the liquid and gaseous states of bulk atomic systems disappears. Then the surface tension on the liquid surface becomes zero. A decrease in the surface energy of small clusters at temperatures of the order of 1100 K has a different nature. Thus, in the framework of the model of a free liquid drop for surface silver clusters, we obtain that these clusters are stable under the conditions of the experiment (and the cluster fragmentation is then absent).

4. MODEL FOR A LIQUID CLUSTER LOCATED ON A PLANAR SURFACE

In analyzing thermodynamics of liquid clusters, we assume in formula (3.1) that the cluster is modeled by

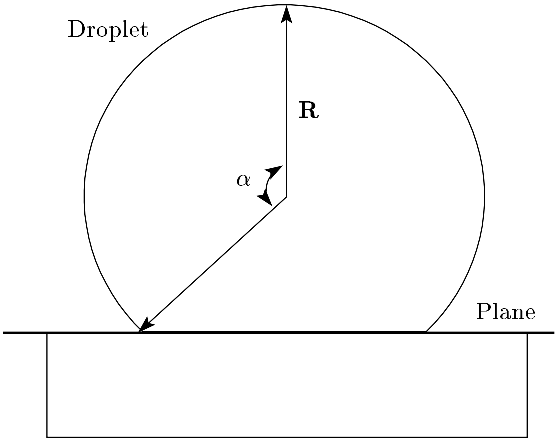

Fig. 3. Parameters of a nanosize liquid drop located on a surface; σ_1 and σ_2 are the surface tensions for the liquid and on the interface

a spherical particle. In reality, a liquid cluster is fastened to a surface, and the interaction between it and the surface at the interface is important both for the cluster shape and for the energy cluster parameters. As a result of this interaction, the cluster loses its spherical shape. Interaction of a liquid drop with a solid surface has been studied from various standpoints [19–23], including microsize and nanosize liquid drops on a solid surface [24] and using various liquid and solid types [25–28].

We use a simple model for the analysis of the behavior of a deposited liquid cluster with the interaction of cluster atoms on a free surface and on the interface taken into account. A schematic form of this drop is given in Fig. 3, where α is the contact angle [29], which is a characteristic of the wettability for this system. We consider a simplified version of a general method for incompressible liquid, where we ignore the gas–liquid and gas–solid interaction, neglect the drop weight, and assume the solid surface to be uniform. Then the behavior of an incompressible liquid drop located on a surface is described by two parameters, the surface tension σ_1 of this liquid and the surface tension σ_2 due to the solid interface. Considering the case of a nonwetting drop, we take $\sigma_2 \leq \sigma_1$, which corresponds to the contact angle $\pi/2 < \alpha < \pi$.

We now verify that the gravitation force can be ignored in this model. For estimation, we take a round drop consisting of n atoms, whose surface energy is $An^{2/3}$ according to formula (3.1). We then compare this energy with the drop weight $U_g = MgR$, where $M = m_0 n$ is the drop mass, m_0 is the mass of an individual atom, and $g = 980$ cm/s^2 is the free-fall acceleration. The round drop radius is $R = r_W n^{1/3}$, where r_W is the Wigner–Seits radius, and the gravitational potential energy in this case is

$$U_g = MgR = Bn^{4/3}, \quad B = m_0 g r_W,$$

and the criterion of the smallness of the drop weight compared to its surface energy is

$$n \ll \left(\frac{A}{B}\right)^{3/2}. \tag{4.1}$$

We apply criterion (4.1) to a silver liquid drop. We have the following parameters of the liquid silver drop [13]:

$$m_0 = 1.8 \cdot 10^{-22} \text{ g}, \quad \varepsilon_0 = 2.87 \text{ eV},$$

$$A = 2.0 \text{ eV}, \quad r_W = 1.66 \,\text{Å}.$$

This gives $B = 1.8 \cdot 10^{-15}$ eV, and criterion (4.1) is satisfied for $R \ll 1$ mm. Because we deal with drop sizes below 100 nm, this criterion is satisfied, and gravitation forces may be ignored.

In the framework of this model, given in Fig. 3, we express the total drop energy E at zero temperature not in the form that follows from formula (3.1) but as

$$E = -\varepsilon_0 n + S_1\sigma_1 + S_2(\sigma_1 - \sigma_2) = \\ = -\varepsilon_0 n + E_{sur}, \quad E_{sur} = S_1\sigma_1 + S_2(\sigma_1 - \sigma_2), \tag{4.2}$$

where ε_0 is the binding energy per atom, S_1 is the area of the free drop surface, S_2 is the area of the interface surface, σ_1 is the liquid surface tension, and σ_2 is the surface tension of the interface corresponding to attraction of drop molecules to the surface. We note that in the limit cases, we have the contact angle $\alpha = \pi$ at $z = \sigma_2/\sigma_1 = 0$, which corresponds to a drop located in a vacuum, and $\alpha = \pi/2$ at $z = 1$ when a drop is transformed into a semi-drop.

Evidently, the minimization of energy (4.2) as a function of the wetting angle α gives the relation between this angle and the ratio of the surface tensions $z = \sigma_2/\sigma_1$. This relation may be obtained in a simpler way from the equality of forces acting on the drop edge. Such a relation is the Young equation [30, 31], which in the conditions of Fig. 3 has the form

$$z \equiv \frac{\sigma_2}{\sigma_1} = 1 + \cos\alpha. \tag{4.3}$$

In comparison with the Young equation [30, 31], we here neglect the interaction of the liquid drop and solid surfaces with the surrounding gas. Equation (4.3) leads to the spherical drop shape $\alpha = \pi$ if the drop is located in a vacuum, i. e., $z = 0$. In the case $\sigma_1 = \sigma_2$ ($z = 1$), we obtain a semi-drop ($\alpha = \pi/2$). It is clear that in the limit $\sigma_1 \ll \sigma_2$, we have $\alpha = 0$, i. e., the drop is converted into a planar film. But we now restrict ourself to the nonwetting case $\sigma_1 \geq \sigma_2$.

We give the relations for the parameters of a surface drop in Fig. 3 that is converted from a spherical drop of a radius R_0. Because the drop contains an incompressible liquid, its volume $V = 4\pi R_0^3/3$ is conserved under the above transformation, and its radius at a given angle α between the surface and the drop edge is equal

$$R = \frac{2^{2/3} R_0}{(1-\cos\alpha)^{2/3}(2+\cos\alpha)^{1/3}} = \frac{2^{2/3} R_0}{x^{2/3}(3-x)^{1/3}}, \quad (4.4)$$

where $x = 1 - \cos\alpha$. The areas of the free drop surface S_1 and the boundary surface with the planar surface S_2 are given by

$$\begin{aligned} S_1 &= 2\pi R^2 (1-\cos\alpha) = \frac{2^{7/3}\pi R_0^2}{x^{1/3}(3-x)^{2/3}}, \\ S_2 &= \pi R^2 \sin^2\alpha = \frac{2^{4/3}\pi R_0^2 (2-x)}{x^{1/3}(3-x)^{2/3}} \end{aligned} \quad (4.5)$$

For the total drop energy determined by formula (4.2), this gives

$$\begin{aligned} E_{sur} &= 4\pi R_0^2 \sigma_1 \Phi(x,z), \quad x = 1-\cos\alpha, \\ z &= \frac{\sigma_2}{\sigma_1}, \quad \Phi(x,z) = \frac{4-x-z(x-2)}{x^{1/3}(6-2x)^{2/3}}. \end{aligned} \quad (4.6)$$

Figure 4 gives the dependences $\Phi(x,z)$ at some values $z < 1$ for a nonwetting liquid.

Figure 5 contains some parameters of a nonwetting drop on a planar surface under optimal conditions as a function of the parameter $z = \sigma_2/\sigma_1$. Specifically, the contact angle α is defined in Fig. 3. The ratio of the height of the drop top h to the drop radius R is given by

$$\frac{h}{R} = 1 - 2\cos\alpha = 2 - z$$

and is shown in Fig. 5. We note that similarly to measurement of the drop distribution over the drop diameter, which is given in Fig. 2 and is obtained with a scanning electron microscope, the distribution over drop heights may be determined with atomic force microscope. Based on such measurements, the parameter $z = \sigma_2/\sigma_1$ can be determined. Next, Fig. 5 shows the dependence on the relative surface tension of the drop $z = \sigma_2/\sigma_1$ for the ratio S_1/S_2 of the area of a free drop surface S_1 to the interface area S_2.

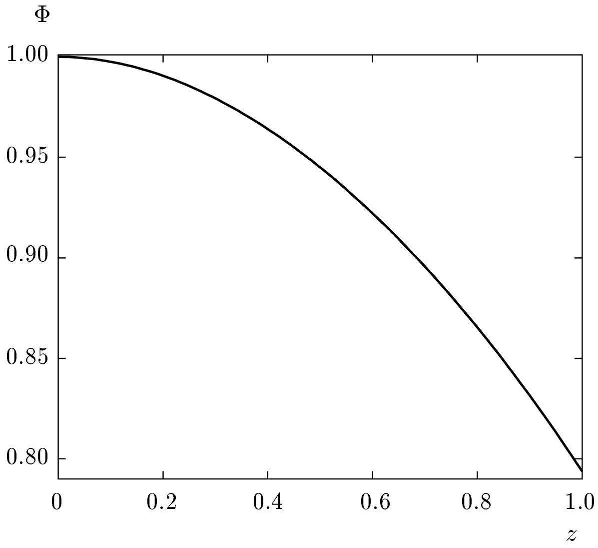

Fig. 4. The function $\Phi(x_{min}, z) = \Phi(z)$ in (4.6) with x_{min} leads to the optimal value of wetting angle α at a given ratio $z = \sigma_2/\sigma_1$. This is the ratio of the surface energy for a drop located on a plane to the energy in the case where this drop is located in a vacuum, as a function of the ratio $z = \sigma_2/\sigma_1$

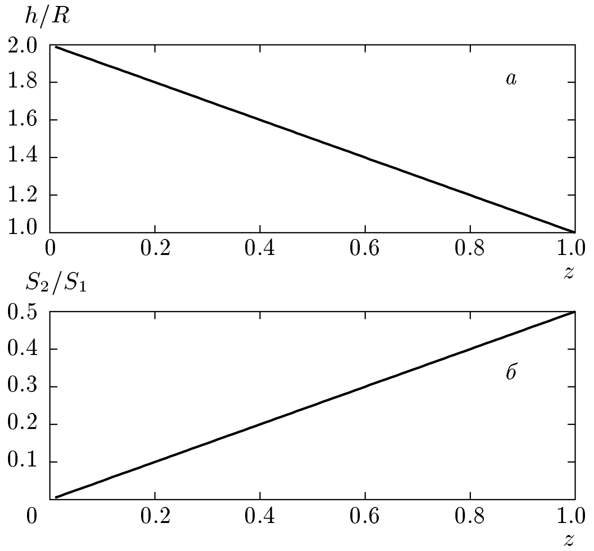

Fig. 5. The reduced parameters of a nanosize liquid drop located on a surface as a function of $z = \sigma_2/\sigma_1$: h/R (a) and S_2/S_1 (b)

We now return to the estimation of the stability of a nanosize liquid silver cluster deposited onto a silicon surface with respect to its fragmentation. Modeling this cluster by a spherical drop, we use Saha formula (3.5) to find the value of its exponent; it is very small because the exponent $Ak^{2/3}/T$ in this formula is large. If we use this drop model with the interaction between the cluster and the substrate taken into account, the value of the parameter A/T decreases, but according to the data in Fig. 4, this decrease does not exceed 20 % for a nonwetting drop. This means that the factor A/T in Saha formula (3.5) remains large for a nonwetting drop, i. e., cluster fragmentation is absent far from the critical point.

5. OSCILLATIONS OF A LIQUID DROP ON A PLANAR SURFACE

We assume that the energy parameters of a liquid cluster allow it to form free fragments, i. e., allow process (3.3) to be thermodynamically profitable. Even in this case, cluster fragmentation may be problematic because it proceeds by fragmentation of a charged drop into two drops of similar sizes (the Rayleigh problem) [32]. On the other hand, cluster fragmentation with the formation of small fragments is possible even under conditions when it is not profitable, but results from dynamic processes due to fluctuations. Therefore, we continue the analysis of the above model of a deposited liquid drop considering its oscillations.

Evidently, a typical frequency of a drop represented in Fig. 3 is given by

$$\omega \sim \sqrt{\frac{E''}{M}},$$

where M is the drop mass and E'' is the second derivative of drop energy (4.2) with respect to the angle α (Fig. 3), and we assume the mass difference for a static and oscillating drop with respect to its shape to be $\Delta M \sim M\Delta\alpha^2$. We note that the total drop mass is conserved in the course of its oscillations, and we let ΔM denote its part located over the drop boundary.

Assuming the drop separation into parts during its oscillations to be connected with this extra part that slides over the stable drop surface, we can estimate the size of drops that can be separated from the stable drop. Indeed, drop oscillations are determined by thermal fluctuations, and the energy of these fluctuations is of the order of T (the drop temperature expressed in energy units). It follows from (4.4) that the typical amplitude of oscillations is given by

$$4\pi R_0^2\sigma_1\Phi''(x,z)\Delta\alpha^2 \sim Tn^{2/3}.$$

Introducing the specific surface energy A in accordance with the relation $An^{2/3} = 4\pi R_0^2\sigma_1$, where n is the total number of drop atoms, and assuming $\Phi''(x,z) \sim 1$, we find that the a typical amplitude of drop oscillations is

$$\Delta\alpha^2 \sim \frac{Tn^{2/3}}{An^{2/3}} \sim \frac{T}{A}.$$

Taking the mass of a separated part to be given by

$$\Delta M \equiv M\Delta n = M\alpha^2,$$

we obtain the number of atoms in the separated drop as

$$\Delta n \sim \frac{T}{A}n.$$

We note that along with symmetric vibrations when the round shape of the drop interface is conserved, there are nonsymmetric oscillations when the center of mass for the interface is shifted. This may lead to the formation of fragments and also to rolling of the liquid drop over the surface. Thus, fluctuations in the droplet vibration may lead to separation of small drop fragments from the drop and displacements or diffusion of this drop over the surface as a result of fluctuations.

We now apply the above estimations to experimental data for silver drops of size $R_0 \approx 35$ nm ($n \approx 9\cdot 10^6$) located on a silicon surface. Taking the temperature $T \approx 0.1$ eV and the specific surface energy $A = 2.0$ eV, we then obtain $\Delta n \approx 4\cdot 10^5$ ($r_0 \approx 12$ nm). It is a rough estimate, which reflects only the nature of the phenomenon under consideration. This estimate shows that fragmentation of a deposited liquid cluster under the experimental conditions may result from fluctuations in cluster oscillations, i. e., this fragmentation develops in the dynamical process under unequilibrium conditions. This means that small cluster debris leave the cluster surface and attach to a surface where they form small clusters.

6. PECULIARITIES OF FRAGMENTATION OF A DROP ON A PLANE SURFACE

According to the experimental data, we observe the fragmentation of a deposited liquid silver clusters at temperatures that are almost an order of magnitude below the critical temperature of bulk silver. Under the experimental conditions, the mass of the formed cluster fragments exceeds the mass of evaporated atoms by almost an order of magnitude, and therefore we can ignore cluster evaporation in the analysis of the fragmentation process. We have analyzed the behavior of the deposited liquid cluster from various standpoints, and summarize the results of this analysis now. We have two possibilities of cluster fragmentation. The first corresponds to thermodynamic equilibrium between the deposited cluster and the fragments, and the second possibility is realized under an unequilibrium process and may be a stage for transition to a new equilibrium.

Based on experimental conditions and thermodynamic equilibrium of a deposited liquid cluster with its fragments, we see that Saha formula (3.5) prohibits fragmentation process (3.3) far from the critical point. The cluster temperature 1073 K at which the cluster fragmentation is observed and the critical temperature approximately equal to 7000 K for bulk silver differ significantly. Nevertheless, we can retain the possibility of a strong decrease in the cluster critical temperature compared to the bulk critical temperature. Indeed, because of an enhanced role of surface properties in the cluster in comparison with the corresponding macroscopic system of bound atoms, all the cluster phenomena are observed at lower temperatures. The melting point for clusters is lower than that for bulk atomic systems [33–37], and this is true for small dielectric [38] and metal clusters [39]. But this decrease in the cluster melting point temperature is usually restricted by a factor of two.

Nevertheless, we can expect that a decrease in the cluster critical temperature compared to the critical temperature of this macroscopic system is stronger than that for the melting point. Indeed, at the critical point, the difference between the liquid and the gas disappears [40–42], i. e., the number of bonds between neighboring atoms becomes equal in both phases. In the case of a bulk system, the transition between the liquid and the gas proceeds throughout the bulk of liquid, while for clusters, this transition primarily relates to the cluster surface. Computer simulation of liquid Lennard–Jones clusters [43, 44] exhibits formation on the cluster surface groups of several weakly bound atoms, and atoms of these groups are bound weakly with the cluster surface. This means that these atom groups may leave the cluster surface and take part in the subsequent formation of surface fragments.

Possibly, the computer simulation of hot liquid clusters in [43, 44] also exhibits the different character of surface processes for small and macroscopic atomic systems. We observe the difference in various cluster processes and phenomena [37, 45–48] compared to those for macroscopic atomic systems. In particular, melting of bulk systems proceeds in a stepwise manner, while the phase coexistence occurs in cluster melting near the melting point [49, 50]. We can also expect a difference in critical phenomena for small and macroscopic atomic systems. Indeed, in the framework of classical thermodynamics [51, 52], we consider the boundary between the liquid and gaseous phases to be compact, for example, consisting of a single atomic layer. The condition for the equilibrium between these phases is that the chemical potential of the gas and liquid are equal; then the rates of atom evaporation transitions from the liquid surface and of atom condensation from the gas to the liquid surface equalize. In this analysis, we assume that the liquid surface is compact, and fluctuations involving groups of a small number of atoms may occur. These fluctuations can lead to formation of small fragments, which is especially important for clusters. We can therefore expect a strong decrease in the cluster critical temperature, although this question remains open.

Another channel of fragment formation corresponds to unequilibrium conditions and can be regarded as a dynamical process. In this case, the deposited liquid clusters and fragments are an intermediate state of the nucleation process similarly to how clusters are an intermediate stage of transition from a gaseous phase to a condensed phase when this condensed phase is thermodynamically profitable [53]. We consider an ensemble of deposited liquid clusters located on a plane surface when they occupy a small part of this surface. If the formation of one large deposited cluster is thermodynamically profitable according to the Saha formula and displacement of individual deposited clusters along the surface is hampered, the cluster growth proceeds via Ostwald ripening [54], as a result of evaporation of some atoms from the cluster surface and their subsequent attachment to large clusters predominantly, as it occurs for island growth on the surface [55, 56]. This is a coalescence process [57], and we can expect that along with individual atoms, it includes small fragments that can join on the surface. This follows from the structure of the cluster surface that contains groups of a small number of weakly bound atoms. Unfortunately, the accuracy of experimental results does not allow us to ascertain the possibility of this mechanism of cluster fragmentation.

7. CONCLUSION

We experimentally observe the fragmentation of deposited liquid clusters, and this process of cluster decay is stronger than atom evaporation from the cluster surface under experimental conditions. This phenomenon contradicts the thermodynamics of macroscopic systems, according to which the surface of liquid clusters is compact. We have considered some theoretical approaches to the nature of this phenomenon, but the restricted experimental information does not allow definitely choosing an appropriate mechanism of this phenomenon. Nevertheless, the above theoretical analysis allows us to outline the way to understanding the nature of the cluster fragmentation phenomenon. Namely, simultaneous measurement of the size distributions of deposited clusters, given in Fig. 2 and made with a scanning electron microscope, and the height distribution for deposited clusters with an atomic force microscope gives the dependence of the contact angle for deposited drops on the temperature and the exposition time. Simultaneously, such measurements give the portion of forming clusters as a result of fragmentation as a function of these parameters. From this, one can derive the nature of the fragmentation phenomenon and its details that will shed light on the different behavior of small cluster and macroscopic particles in surface processes.

This work was supported by the Deutsche Forschungs-Gemeinschaft (grant № SFB/TRR 24) and by the RFBR (grant № 09-02-00108a).

REFERENCES

1. C. Binns, Surf. Sci. Rep. **44**, 1 (2001).

2. K. Shintani, Y. Taniguchi, and S. Kameoka, J. Appl. Phys. **95**, 8207 (2004).

3. S. Y. Liau et al., Lett. Appl. Microbiol. **25**, 279 (1997).

4. A. Gupta and S. Silver, Nature Biotechnol. **16**, 888 (1998).

5. K. Nomiya et al., J. Inorg. Biochem. **98**, 46 (2004).

6. J. R. Morones et al., Nanotechnology **16**, 2346 (2005).

7. I. Shyjumon, M. Gopinadhan, C. A. Helm, B. M. Smirnov, and R. Hippler, Thin Solid Films **500**, 41 (2006).

8. I. Shyjumon, M. Gopinadhan, O. Ivanova, M. Quaas, H. Wulff, C. A. Helm, and R. Hippler, Eur. Phys. J. D **37**, 409 (2006).

9. B. M. Smirnov, I. Shyjumon, and R. Hippler, Phys. Rev. E **77**, 066402 (2007).

10. S. R. Bhattacharyya, T. K. Chini, D. Datta, R. Hippler, I. Shyjumon, and B. M. Smirnov, Zh. Eksp. Teor. Fiz. **134**, 1181 (2008).

11. S. R. Bhattacharyya, D. Datta, I. Shyjumon, B. M. Smirnov, T. K. Chini, D. Ghose, and R. Hippler, J. Phys. D **42**, 035306 (2009).

12. S. Ino, J. Phys. Soc. Jpn. **27**, 941 (1969).

13. B. M. Smirnov, *Clusters and Small Particles in Gases and Plasmas*, Springer, New York (1999).

14. E. P. Wigner and F. Seits, Phys. Rev. **46**, 509 (1934).

15. E. P. Wigner, Phys. Rev. **46**, 1002 (1934).

16. L. D. Landau and E. M. Lifshitz, *Statistical Physics, Vol. 1*, Pergamon Press, Oxford (1980).

17. B. M. Smirnov, *Reference Data on Atomic Physics and Atomic Processes*, Springer, Heidelberg (2008).

18. V. E. Fortov, A. G. Khrapak, and I. T. Jakubov, *Physics of Nonideal Plasma*, Fizmatlit, Moscow (2004).

19. J. J. Bikerman, *Surface Chemistry*, Academic Press, New York (1958).

20. D. P. Woodruff, *The Solid-Liquid Interface*, Academic Press, London (1973).

21. A. W. Adamson, *Physical Chemistry of Surfaces*, Wiley, New York (1976).

22. J. N. Israelachvili, *Intermolecular and Surface Forces*, Academic Press, London (1989).

23. M. E. Schrader and G. I. Loeb, *Modern Approaches to Wettability. Theory and Applications*, Plenum Press, New York (1992).

24. P. L. Gai and E. D. Boyes, *Electron Microscopy in Heterogeneous Catalysis*, Inst. Phys. Publ. Ltd, London (2003).

25. P. G. de Gennes, Rev. Mod. Phys. **57**, 827 (1985).

26. C. Isenberg, *The Science of Soap Films and Soap Bubles*, Dover, New York (1992).

27. P. G. de Gennes, *Soft Interfaces*, Cambr. Univ. Press, Cambridge (1994).

28. N. Eustathopoulos, M. G. Nicholas, and B. Drevet, *Wettability at High Temperatures*, Pergamon Press, Oxford (1999).

29. http://en.wikipedia.org/wiki/Wetting.

30. T. Young, Phil. Trans. Roy. Soc. **1**, 84 (1805).

31. T. Young, Proc. Roy. Soc. **95**, 65 (1805).

32. L. D. Landau and E. M. Lifshitz, *Electrodynamics of Continuous Media*, Pergamon Press, Oxford (1984).

33. T. P. Martin, U. Näher, H. Schaber, and U. Zimmermann, J. Chem. Phys. **100**, 2322 (1994).

34. T. P. Martin, Phys. Rep. **273**, 199 (1996).

35. M. Schmidt, R. Kusche, W. Kronmüller, B. von Issendorf, and H. Haberland, Phys. Rev. Lett. **79**, 99 (1997).

36. M. Schmidt, R. Kusche, B. von Issendorf, and H. Haberland, Nature **393**, 238 (1998).

37. B. M. Smirnov and R. S. Berry, *Phase Transitions in Simple Atomic Systems*, Springer, Heidelberg (2007).

38. T. L. Beck, J. Jellinek, and R. S. Berry, J. Chem. Phys. **87**, 545 (1987).

39. H. Arslan and M. H. Güven, New J. Phys. **7**, 60 (2005).

40. E. Stanley, *Introduction to Phase Transitions and Critical Phenomena*, Oxford Univ. Press, New York (1971).

41. A. R. Ubbelohde, *The Molten State of Matter*, Wiley, Chicester (1978).

42. C. Domb, *The Critical Point*, Taylor and Francis, London (1996).

43. D. I. Zhukhowitskii, J. Chem. Phys. **125**, 234701 (2006).

44. D. I. Zhukhowitskii, J. Chem. Phys. **129**, 194511 (2008).

45. *Clusters of Atoms and Molecules*, ed. by H. Haberland, Springer, New York (1994).

46. *Theory of Atomic and Molecular Clusters*, ed. by J. Jellinek, Springer, Berlin (1999).

47. *Metal Clusters*, ed. by W. Ekardt, Wiley, New York (1999).

48. D. J. Wales, *Energy Landscapes*, Cambr. Univ. Press, Cambridge (2003).

49. J. Jellinek, T. L. Beck, and R. S. Berry, J. Chem. Phys. **84**, 2783 (1986).

50. R. S. Berry, Chem. Rev. **93**, 2379 (1993).

51. J. W. Gibbs, Trans. Conn. Acad. Arts. Sci. **3**, 108 (1875); **3**, 343 (1878).

52. J. W. Gibbs, *The Collected Works*, Longmans and Green, New York (1928).

53. B. M. Smirnov, *Principles of Statistical Physics*, Wiley, Berlin (2006).

54. W. Ostwald, Z. Phys. Chem. **34**, 495 (1900).

55. B. Lewis and J. C. Anderson, *Nucleation and Growth of Thin Films*, Academic Press, New York (1978).

56. S. A. Kukushkin and V. V. Slezov, *Disperse Systems on Solid Surfaces*, Nauka, Petersburg (1996).

57. L. D. Landau and E. M. Lifshitz, *Statistical Physics, Vol. 2*, Pergamon Press, Oxford (1980).